https://doi.org/10.5194/acp-2020-300
Preprint. Discussion started: 6 April 2020

Atmospheric Chemistry and Physics Discussions

Dilution impacts on smoke aging: Evidence in BBOP data

Anna L. Hodshire[1], Emily Ramnarine[1], Ali Akherati[2], Matthew L. Alvarado[3], Delphine K. Farmer[4], Shantanu H. Jathar[2], Sonia M. Kreidenweis[1], Chantelle R. Lonsdale[3], Timothy B. Onasch[5], Stephen R. Springston[6], Jian Wang[6,a], Yang Wang[7,b], Lawrence I. Kleinman[6], Arthur J. Sedlacek III[6], Jeffrey R. Pierce[1]

[1] Department of Atmospheric Science, Colorado State University, Fort Collins, CO 80523, United States
[2]Department of Mechanical Engineering, Colorado State University, Fort Collins, CO 80523, United States
[3]Atmospheric and Environmental Research, Inc., Lexington, MA 02421, United States
[4]Department of Chemistry, Colorado State University, Fort Collins, CO 80523, United States
[5]Aerodyne Research Inc., Billerica, MA 01821, United States
[6]Environmental and Climate Sciences Department, Brookhaven National Laboratory, Upton, NY 11973, United States
[7]Center for Aerosol Science and Engineering, Washington University, St. Louis, MO 63130, United States
[a]Now at Center for Aerosol Science and Engineering, Washington University, St. Louis, MO 63130, United States
[b]Now at Department of Civil, Architectural and Environmental Engineering, Missouri University of Science and Technology, Rolla, Missouri 65409, United States

Correspondence to: Anna L. Hodshire (Anna.Hodshire@colostate.edu)

Abstract. Biomass burning emits vapors and aerosols into the atmosphere that can rapidly evolve as smoke plumes travel downwind and dilute, affecting climate- and health-relevant properties of the smoke. To date, theory has been unable to explain variability in smoke evolution. Here, we use observational data from the BBOP field campaign and show that initial smoke concentrations can help predict changes in smoke aerosol aging markers, number, and diameter. Because initial field measurements of plumes are generally >10 minutes downwind, smaller plumes will have already undergone substantial dilution relative to larger plumes. However, the extent to which dilution has occurred prior to the first observation is not a measurable quantity. Hence, initial observed concentrations can serve as an indicator of dilution, which impacts photochemistry and aerosol evaporation. Cores of plumes have higher concentrations than edges. By segregating the observed plumes into cores and edges, we infer that particle aging, evaporation, and coagulation occurred before the first measurement, and we find that edges generally undergo higher increases in oxidation tracers, more decreases in semivolatile compounds, and less coagulation than the cores.

https://doi.org/10.5194/acp-2020-300
Preprint. Discussion started: 6 April 2020


Atmospheric Chemistry and Physics Discussions

1 Introduction

Smoke from biomass burning is a major source of atmospheric primary aerosol and vapors (Akagi et al., 2011; Gilman et al., 2015; Hatch et al., 2015, 2017; Jen et al., 2019; Koss et al., 2018; Reid et al., 2005; Yokelson et al., 2009), influencing air quality, local radiation budgets, cloud properties, and climate (Carrico et al., 2008; O'Dell et al., 2019; Petters et al., 2009; Ramnarine et al., 2019; Shrivastava et al., 2017), as well as the health of smoke-impacted communities (Ford et al., 2018; Gan et al., 2017; Reid et al., 2016). Vapors and particles emitted from fires can rapidly evolve as smoke travels downwind (Adachi et al., 2019; Akagi et al., 2012; Bian et al., 2017; Cubison et al., 2011; Hecobian et al., 2011; Hodshire et al., 2019a, 2019b; Jolleys et al., 2012, 2015; Konovalov et al., 2019; May et al., 2015; Noyes et al., 2020; Sakamoto et al., 2015), diluting and entraining regional background air. Fires span an immense range in size, from small agricultural burns, which may be only a few m^2 in total area and last a few hours, to massive wildfires, which may burn 10,000s of km^2 over the course of weeks (Andela et al., 2019). This range in size leads to variability in initial plume size and dilution, as large, thick plumes dilute more slowly than small, thin plumes for similar atmospheric conditions (Akagi et al., 2012; Bian et al., 2017; Cubison et al., 2011; Hecobian et al., 2011; Hodshire et al., 2019a, 2019b; Jolleys et al., 2012, 2015; Konovalov et al., 2019; May et al., 2015; Sakamoto et al., 2015)). Plumes can dilute unevenly, with edges of the plume mixing in with surrounding air more rapidly than the core of the plume. Variability in dilution leads to variability in the evolution of smoke emissions as instantaneous plume thickness will control shortwave fluxes (and thus photolysis rates and oxidant concentrations), gas-particle partitioning, and particle coagulation rates ((Akagi et al., 2012; Bian et al., 2017; Cubison et al., 2011; Hecobian et al., 2011; Hodshire et al., 2019a, 2019b; Jolleys et al., 2012, 2015; Konovalov et al., 2019; May et al., 2015; Sakamoto et al., 2015), (Garofalo et al., 2019), (Ramnarine et al., 2019; Sakamoto et al., 2016)). Thus, capturing variability in plume thickness and dilution between fires and within fires can aid in understanding how species change within the first few hours of emission for a range of plume sizes.

The evolution of total particulate matter (PM) or organic aerosol (OA) mass from smoke has been the focus of many studies, as PM influences both human health and climate. Secondary organic aerosol (SOA) production may come about through oxidation of gas-phase volatile organic compounds (VOCs) that can form lower-volatility products that partition to the condensed phase (Jimenez et al., 2009; Kroll and Seinfeld, 2008). SOA formation may also arise from heterogeneous and multi-phase reactions in both the organic and aqueous phases (Jimenez et al., 2009; Volkamer et al., 2009). In turn, oxidant concentrations depend on shortwave fluxes (Tang et al., 1998; Tie, 2003; Yang et al., 2009). Smoke particles contain semivolatile organic compounds (SVOCs) (Eatough et al., 2003); (May et al., 2013), which may evaporate off of particles as the plume becomes more dilute (Formenti et al., 2003; Huffman et al., 2009; May et al., 2013), leading to losses in total aerosol mass. Field observations of smoke PM and OA mass normalized for dilution (e.g. through an inert tracer such as CO) report that for near-field (<24 hours) physical aging, net PM or OA mass can increase (Cachier et al., 1995; Formenti et al., 2003; Liu et al., 2016; Nance et al., 1993; Reid et al., 1998; Vakkari et al., 2014, 2018; Yokelson et al., 2009), decrease (Akagi et al., 2012; Hobbs et al., 2003; Jolleys et al., 2012, 2015; May et al., 2015), or remain nearly

https://doi.org/10.5194/acp-2020-300
Preprint. Discussion started: 6 April 2020


Atmospheric Chemistry and Physics Discussions

constant (Brito et al., 2014; Capes et al., 2008; Collier et al., 2016; Cubison et al., 2011; Forrister et al., 2015; Garofalo et al., 2019; Hecobian et al., 2011; Liu et al., 2016; May et al., 2015; Morgan et al., 2019; Sakamoto et al., 2015; Sedlacek et al., 2018; Zhou et al., 2017). It is theorized that both losses and gains in OA mass are likely happening concurrently in most plumes through condensation and evaporation (Bian et al., 2017; Hodshire et al., 2019a, 2019b; May et al., 2015), with the balance between the two determining whether net increases or decreases or no change in mass occurs during near-field aging. However, there is currently no reliable predictor of how smoke aerosol mass (normalized for dilution) may change for a given fire.

Evolution of total aerosol number, size, and composition is critical in improving quantitative understanding of how biomass burn smoke plumes impact climate. These impacts include smoke aerosols' abilities to both act as cloud condensation nuclei (CCN) and to scatter/absorb solar radiation, each of which is determined by particle size and composition (Albrecht, 1989; Petters and Kreidenweis, 2007; Seinfeld and Pandis, 2006; Twomey, 1974; Wang et al., 2008). Particles can increase or decrease in size as well as undergo compositional changes through condensation or evaporation of vapors. In contrast, coagulation always decreases total number concentrations and increases average particle diameter; plumes with higher concentrations will undergo more coagulation than those with lower concentrations (Sakamoto et al., 2016).

Being able to predict smoke aerosol mass, number, size, and composition accurately is an essential component in constraining the influence of fires on climate, air quality, and health. Fires in the western United States region are predicted to increase in size, intensity, and frequency (Dennison et al., 2014; Ford et al., 2018; Spracklen et al., 2009; Yue et al., 2013). In response, several large field campaigns have taken place in the last 7 years examining wildfires in this region (Kleinman and Sedlacek 2016; Garofalo et al. 2019). Here, we present smoke plume observations from the Biomass Burning Observation Project (BBOP) campaign of aerosol properties from five research flights sampling wildfires downwind in seve[illegible]udo-Lagrangian sets of transects to investigate aging of OA mass and oxidation, and aerosol number and mean diameter. A range of initial plume OA mass concentrations were captured within these flights and sufficiently fast (1 second) measurements of aerosols and key vapors were taken. We segregate each transect into edge, core, or intermediate regions of the plume and examine aerosol properties within the context of both the location within the plume (edge, core, or intermediate) and the initial OA mass loading of the given location, with the differences in aerosol loading serving as a proxy for differences in dilution rates, as the extent to which dilution has occurred prior to the first observation is not a measurable quantity. We create mathematical fits for predicting OA oxidation markers and mean particle diameter given initial plume mass and physical age (time) of the smoke. These fits may be used to evaluate other smoke datasets and assist in building parameterizations for regional and global climate models to better-predict smoke aerosol climate and health impacts.

https://doi.org/10.5194/acp-2020-300
Preprint. Discussion started: 6 April 2020


Atmospheric Chemistry and Physics Discussions

2 Methods

The BBOP field campaign occurred in 2013 and included a deployment of the United States Department of Energy Gulfstream 1 (G-1) research aircraft in the Pacific Northwest region of the United States (Kleinman and Sedlacek, 2016; Sedlacek et al., 2018) from June 15 to September 13. We analyze five cloud-free BBOP research flights that had seven total sets of across-plume transects that followed the smoke plume downwind in a pseudo-Lagrangian manner (see Figs. S1-S6 for examples; Table S1) from approximately 15 minutes after emission to 2-4 hours downwind (Kleinman and Sedlacek, 2016). The G-1 sampling setup is described in (Kleinman and Sedlacek, 2016; Sedlacek et al., 2018; Kleinman et al., 2020).

Number size distributions were obtained with a Fast-integrating Mobility Spectrometer (FIMS), providing particle size distributions nominally from ~20-350 nm (Kulkarni and Wang, 2006; Olfert and Wang, 2009); data was available between 20-[illegible]m for the flights used in this study. A Soot Photometer Aerosol Mass Spectrometer (SP-AMS) provided organic and inorganic (sulfate, chlorine, nitrate, ammonium) aerosol masses, select fractional components (the fraction of the AMS OA spectra at a given mass-to-charge ratio) (Onasch et al., 2012), and elemental analysis (O/C and H/C) (Aiken et al., 2008; Canagaratna et al., 2015). We use the f_{60} and f_{44} fractional components (the mass concentrations of m/z 60 and 44 normalized by the total OA mass concentration) and O/C and H/C elemental ratios of OA as tracers of smoke and oxidative aging. Elevated f_{60} values are indicative of "levoglucosan-like" species (levoglucosan and other molecules that similarly fragment in the AMS) (Aiken et al., 2009; Cubison et al., 2011; Lee et al., 2010) and are shown to be tracers of smoke primary organic aerosol (POA) (Cubison et al., 2011). The f_{44} fractional component (arising from primarily CO_2+ as well as some acid groups;) is indicative of SOA arising from oxidative aging (Alfarra et al., 2004; Cappa and Jimenez, 2010; Jimenez et al., 2009; Volkamer et al., 2006). Fractional components f_{60} and f_{44} have been shown to decrease and increase with photochemical aging, respectively, likely due to both evaporation and/or oxidation of semivolatile f_{60}-containing species and addition of oxidized f_{44}-containing species (Alfarra et al., 2004; Huffman et al., 2009). O/C tends to increase with oxidative aging (Decarlo et al., 2008) whereas H/C ranges from increasing to decreasing with oxidative aging, depending on the types of reactions occurring (Heald et al., 2010). Thus, tracking H/C with aging may provide clues upon the types of reactions that may be occuring. A Single-Particle Soot Photometer (SP2; Droplet Measurement Technologies) was used to measure refractory black carbon (rBC) through laser-induced incandescence (Moteki and Kondo, 2010; Schwarz et al., 2006). An Off-Axis Integrated-Cavity Output Spectroscopy instrument (Los Gatos, Model 907) provided CO measurements. An SPN1 radiometer (Badosa et al., 2014; Long et al., 2010) provided total shortwave irradiance. The supporting information includes more details on the instruments used.

To determine the contribution of species X from smoke, the background concentration of X is subtracted off and normalized by background-corrected CO (ΔCO), which is inert on timescales of near-field aging (Yokelson et al., 2009), to correct for dilution. Increases or decreases of ΔX/ΔCO with time indicate whether the total amount of X in the plume has increased or decreased since time of emission. We background correct the number size distribution, OA, O, H, C, and rBC data in this manner by determining an average regional background for each species by using the lowest 10% of the CO data

https://doi.org/10.5194/acp-2020-300
Preprint. Discussion started: 6 April 2020


Atmospheric Chemistry and Physics Discussions

for a given flight with a similar altitude, latitude, and longitude as the smoke plume (excluding data from flying to and from the fire). Elemental O, H, and C are calculated using the O/C and H/C and OA data from the SP-AMS, allowing us to calculate ΔO/ΔC and ΔH/ΔC. We also background-correct f_{60} and f_{44} (using the mass concentrations of m/z 60, m/z 44, and OA inside and outside of the plume), we but do not normalize by CO due to these values already being normalized by OA. We only consider data to be in-plume if the absolute CO >= 150 ppbv, as comparisons of CO and the number concentration show that in-plume data has CO >150 ppbv and out-of-plume (background) data has CO < 150 ppbv. This threshold appears to be capturing clear plume features while excluding background air (Figs. S7-S11); we perform sensitivity analyses of our results to our assumptions about background and in-plume values in Section 3.

From the FIMS, we examine the background-corrected, normalized number concentrations of particles with diameters between 40-262 nm, $\Delta N_{40\text{-}262\ nm}/\Delta CO$. $\Delta N_{40\text{-}262\ nm}/\Delta CO$ allows us to exclude potential influence of fresh nucleation upon the total number concentrations, as the bulk of observed newly formed particles observed fell below 40 nm (Figs. S7-S11). Smoke plumes contain particles with diameters larger than 262 nm (Janhäll et al., 2009), and so although we cannot provide total number concentrations, we can infer how the evolution of $\Delta N_{40\text{-}262\ nm}/\Delta CO$ will impact number concentrations overall. We also obtain an estimate of how the mean diameter between 40-262 nm, $\overline{D_p}$, changes with aging through:

$$\overline{D_p} = \frac{\Sigma N_i * D_{p,i}}{\Sigma N_i} \qquad \text{Eq. 1}$$

Where N_i and $D_{p,i}$ are the number concentration and geometric mean diameter within each FIMS size bin, respectively.

All of the data are provided at 1 Hz and all but the SP-AMS fractional component data are available on the DOE ARM web archive (https://www.arm.gov /research/campaigns/aaf2013bbop). As the plane traveled at ~100 m s^{-1} on average, data were collected every 100 m across the plume. The instruments used here had a variety of time lags (all <10 seconds) relative to a TSI 3563 nephelometer used as reference. The FIMS also showed an additional lag in flushing smoky air with cleaner air when exiting the plume with maximum observed flushing timescales around 30 seconds, but generally less (Fig. S12). To test if these lags impact our results, we perform an additional analysis where we only consider the first half of each in-plume transect, when concentrations are generally rising with time (Figure S12-S13), and our main conclusions are unaffected. We do not test the impacts of other timelags.

We use MODIS Terra and Aqua fire and thermal anomalies detection data to determine fire locations (Giglio et al., 2006, 2008) and estimate the fire center to be the approximate center of all clustered MODIS detection points for a given sampled fire (Figs. S1-S6). Depending upon the speed of the fire front, the true fire location and center at the time of sampling is likely different than the MODIS estimates. To estimate the physical age of the plume, we use the estimated fire center as well as the FIMS number distribution to determine an approximate centerline of the plume as the smoke travels downwind (Figs. S1-S6) and use mean wind speed and this estimated centerline to get an estimated physical age for each

https://doi.org/10.5194/acp-2020-300
Preprint. Discussion started: 6 April 2020


Atmospheric Chemistry and Physics Discussions

transect. We did not propagate uncertainty in fire location, wind speed, or centerline through to the physical age, which is a limitation of this study.

3 Results and discussion (as Heading 1)

As a case example, we examine the aging profiles of smoke from the Colockum fire during the first set of pseudo-Lagrangian transects on flight 730b (Table S1). Fig. 1 provides ΔOA/ΔCO, ΔrBC/ΔCO Δf_{60}, Δf_{44}, ΔH/ΔC, ΔO/ΔC, $\Delta N_{40\text{-}262\ nm}$/ΔCO, and $\overline{D_p}$ as a function of the estimated physical age; Figs. S14-S18 provide this information for the other pseudo-Lagrangian transect sets studied. We have divided each transect into four regions: between the 5-15 (edge), 15-50 (intermediate, outer), 50-90 (intermediate, inner), and 90-100 (core) percentile of ΔCO within each transect. Fig. 1 shows the edge and core data, both averaged per transect, with Figs. S14-18 providing all four percentile bins for each flight. These percentile bins correspond with the thinnest to thickest portions of the plume, respectively, and if a fire has uniform emissions ratios across all regions and dilutes evenly downwind, these percentile bins would correspond to the edges, intermediate regions, and the core of the diluting plume. We use this terminology in this study but note that uneven emissions, mixing, and/or dilution lead to the percentile bins not corresponding physically to our defined regions in some cases. However, the lowest two ΔCO bins tend more towards the physical edges of the plume and the highest two tend more towards the physical center of the plume (Figs. S2-S6). We do not use the data from the lowest 5% of ΔCO to reduce uncertainty at the plume-background boundary. We do not know where the plane is vertically in the plume, which is a limitation as vertical location will also impact the amount of solar flux able to penetrate through the plume.

Fig. 1 shows that ΔOA/ΔCO and ΔrBC/ΔCO vary little with age. A true Lagrangian flight with the aircraft sampling the same portion of the plume and no measurement artifacts (e.g. coincidence errors at high concentrations) would have a constant ΔrBC/ΔCO for each transect. This flight and other flights studied here have slight variations in ΔrBC/ΔCO (Fig. 1; Figs. S14-S18), which may be indicative of deviations from a Lagrangian flight path with temporal variations in emission and/or measurement uncertainties. For this flight, Δf_{60} changes little (~±6% between edge and core) while Δf_{44} increases slightly (~8% for both edge and core) with age, with edges showing the highest Δf_{44}. ΔH/ΔC decreases while ΔO/ΔC increases with the edges showing higher values of ΔO/ΔC. Mean aerosol diameter increases and normalized number concentration decreases between 40-262 nm with aging. The decrease in number concentration is presumably due to coagulation, as little dry deposition would occur within these timescales (<2.5 hours). These trends are discussed for all flights in the following sections.

3.1 Organic aerosol aging: ΔOA/ΔCO, Δf_{60}, Δf_{44}, ΔH/ΔC, and ΔO/ΔC

Fig. 2a-e show available ΔOA/ΔCO, Δf_{60}, Δf_{44} ΔH/ΔC, and ΔO/ΔC edge and core data versus physical age for each transect for each flight of this study, colored by the mean ΔOA within a ΔCO percentile bin from the transect closest to

https://doi.org/10.5194/acp-2020-300
Preprint. Discussion started: 6 April 2020


Atmospheric Chemistry and Physics Discussions

the fire, $\Delta OA_{initial}$. We show the 5-15 (edge) and 90-100 (core) ΔCO percentile bins here; Fig. S19 shows the same information for all four ΔCO percentiles. We note that although some of the physical ages appear to be at ~0 hours, this is from a limitation of our physical age estimation method (Sect. 2), as no flights captured data before ~15 minutes after emission (Kleinman et al., 2016). Also included in Fig. 2 are the Spearman rank-order correlation tests (hereafter Spearman tests) that show correlation coefficients (R) with initial plume OA mass, $\Delta OA_{initial}$ ($R_{\Delta OA,initial}$), and physical age (R_{age}) against each variable (for the correlations with $\Delta OA_{initial}$, all transects in a set are given the same $\Delta OA_{initial}$ value). Figs. S13, S19-S21 show the same details as Fig. 2 but provide sensitivity tests to potential FIMS measurement artifacts (Fig. S13) and our assumed background CO and ΔCO percentile spacing (Figs. S19-S21). Although these Figs. show slight variability, the findings discussed below remain robust and we constrain the rest of our discussion to the FIMS measurements and background and ΔCO percentile spacings used in Fig. 2.

In general, both the cores and edges show little change in ΔOA/ΔCO with physical aging, with $R_{\Delta OA,initial}$ and R_{age} both at 0.03 (the absolute variability is dominated by differences between plumes). While the observed trends in ΔOA/ΔCO with aging are small, Δf_{60} and Δf_{44} show clear signs of changes with aging, consistent with previous studies (Cubison et al., 2011; Garofalo et al., 2019; May et al., 2015). Spearman tests on physical age vs. Δf_{60} and Δf_{44} give R_{age} values of -0.25 and 0.54, respectively. Δf_{60} generally decreases with plume age, consistent with the hypotheses that Δf_{60} may be evaporating off through heterogeneous oxidation and/or has a decreasing fractional contribution due to condensation of other compounds. In contrast, Δf_{44} generally increases with age for all plumes with available data, and hence it would appear that for plumes with little change in ΔOA/ΔCO, evaporation of f_{60}-containing compounds is roughly balanced by condensation of more-oxidized compounds, including those that contain f_{44}, suggesting the possibility that heterogeneous or particle-phase oxidation that would alter the balance of Δf_{60}, and Δf_{44}. However, estimates of heterogeneous mass losses indicate that after three hours of aging for a range of OH concentrations and reactive uptake coefficients over 90% of aerosol mass remains (Fig. S23; see SI text S2 for more details on the calculation).

Two more important features of Δf_{60} and Δf_{44} can be seen within Fig. 2: (1) Δf_{60} and Δf_{44} depend on $\Delta OA_{initial}$ ($R_{\Delta OA,initial}$ = 0.38 and -0.5, respectively), with more concentrated plumes having consistently higher Δf_{60} and lower Δf_{44}. (2) Differences in Δf_{60} and Δf_{44} for the nearest-to-source measurements indicate that evaporation and/or chemistry likely occurred before the time of these first measurements (assuming that emitted Δf_{60} and Δf_{44} do not correlate with $\Delta OA_{initial}$). The amounts of evaporation and/or chemistry depend on $\Delta OA_{initial}$, with higher rates of evaporation and chemistry occurring for lower values of $\Delta OA_{initial}$. This result is consistent with the hypothesis that aircraft observations are missing evaporation and chemistry prior to the first aircraft observation (Hodshire et al., 2019b). The differences in $\Delta OA_{initial}$ between plumes may be due to different emissions fluxes (e.g., due to different fuels or combustion phases), or plume widths, where larger/thicker plumes dilute more slowly than smaller/thinner plumes; these larger plumes have been predicted to have less evaporation and may undergo relatively less photooxidation (Bian et al., 2017; Hodshire et al., 2019a, 2019b).

(Garofalo et al., 2019) segregated smoke data from the WE-CAN field campaign by distance from the center of a given plume and showed that the edges of one of the fires studied have less f_{60} and more f_{44} (not background-corrected) than

https://doi.org/10.5194/acp-2020-300
Preprint. Discussion started: 6 April 2020


Atmospheric Chemistry and Physics Discussions

the core of the plume. Similarly, we find that the 730b flight shows a very similar pattern in f_{60} and f_{44} (Figs. S24-S25) to that shown in (Garofalo et al., 2019) (their Fig. 6). The 821b and 809a flights also hint at elevated f_{44} and decreased f_{60} at the edges but the remaining plumes do not show a clear trend from edge to core in f_{60} and f_{44}. This could be as CO concentrations (and thus presumably other species) do not evenly increase from the edge to the core for many of the plume transects studied (Figs. S2-S6). We do not have UV measurements that allow us to calculate photolysis rates but the in-plume shortwave measurements in the visible show a dimming in the fresh cores that has a similar pattern to f_{44} and the inverse of f_{60} (Fig. S26; the rapid oscillations in this figure could be indicative of sporadic cloud cover above the plumes).

We also plot core and edge ΔH/ΔC and ΔO/ΔC as a function of physical age (Fig. 2d-e). Similar to Δf_{44}, ΔO/ΔC increases with physical age and is well correlated to both physical age and $\Delta OA_{initial}$ (R_{age} = 0.61 and $R_{\Delta OA,initial}$ = -0.42). Conversely, ΔH/ΔC tends to be fairly constant or slightly decreasing with physical age and is poorly correlated to physical age and $\Delta OA_{initial}$. A Van Krevelen diagram of ΔH/ΔC versus ΔO/ΔC (Fig. S27) indicates that oxygenation reactions or a combination of oxygenation and hydration reactions are likely dominant (Heald et al., 2010); however, without further information, we cannot conclude which reactions are occurring.

Both physical age and $\Delta OA_{initial}$ appear to influence Δf_{60}, Δf_{44}, and ΔO/ΔC: oxidation reactions and evaporation from dilution occur with aging, and the extent of photochemistry and dilution should depend on plume thickness. Being able to predict biomass burning aerosol aging parameters can provide a framework for interstudy-comparisons and can aid in modeling efforts. We construct mathematical fits for predicting Δf_{60}, Δf_{44}, and ΔO/ΔC:

$$X = a\ log_{10}(\Delta OA_{initial}) + b\ (Physical\ age)\ + c \qquad \text{Eq. 2}$$

where X is Δf_{60}, Δf_{44}, or ΔO/ΔC and a, b, and c are fit coefficients. The measured vs. fit data and values of a, b, and c are shown in Fig. 3a-c. The Pearson and Spearman coefficients of determination (R^2_p and R^2_s, respectively) are also summarized in Fig. 3 and indicate moderate goodness of fits (R^2 between 0.21-0.25 for Δf_{60}, between 0.53-0.58 for Δf_{44}, and between 0.41-0.58 for ΔO/ΔC). Although no models that we are aware of currently predict aerosol fractional components (e.g. f_{60} or f_{44}), O/H and H/C are predicted by some models (e.g., (Cappa and Wilson, 2012) and these fit parameters may assist in biomass burning modeling.

Other functional fits were explored (Figs. S28-S29), with

$$ln(\Delta X) = a\ ln(\Delta OA_{initial}) + b\ ln(Physical\ age)\ + c \qquad \text{Eq. 3}$$

(Fig. S28) and $\Delta N_{initial}$ in the place of $\Delta OA_{initial}$ in Eq. 2 (Fig. S29) providing similar fits for Δf_{60} and Δf_{44}. Aged Δf_{60} and Δf_{44} show scatter, limiting the predictive skill of measurements available from BBOP. The scatter is likely to variability in emissions due to source fuel or combustion conditions, instrument noise and response under large concentration ranges encountered in these smoke plumes, inhomogeneous mixing within the plume, variability in background concentrations not

https://doi.org/10.5194/acp-2020-300
Preprint. Discussion started: 6 April 2020


Atmospheric Chemistry and Physics Discussions

captured by our background correction method, inaccurate characterizations of physical age due to variable wind speed, and deviations from a true Lagrangian flight path. There may be another variable not available to us from the BBOP data that aids this prediction, such as photolysis rates. We encourage these fits to be tested out with further data sets and modeling.

3.2 Aerosol size distribution properties: $\Delta N_{40\text{-}262\ nm}/\Delta CO$ and $\overline{D_p}$

The observations of the normalized number concentration between 40-262 nm, $\Delta N_{40\text{-}262\ nm}/\Delta CO$ (Fig. 2f), show that plume edges and cores generally show decreases in $\Delta N_{40\text{-}262\ nm}/\Delta CO$ with physical age, with $R_{age} = -0.25$. The plume edges and cores with the highest initial ΔOA generally have lower normalized number concentrations by the time of the first measurement, and the edges generally have higher initial normalized number concentrations than the cores, potentially due to differences in coagulation rates. A few dense cores have normalized number concentrations comparable or higher than the thinner edges, leading to no correlation with $\Delta OA_{initial}$. We note that variability in number emissions (due to e.g. burn conditions) adds noise not captured by the R values.

The mean particle size between 40-262 nm, $\overline{D_p}$ (Eq. 1), is shown to increase with aging (Fig. 2g) for all plumes ($R_{age} = 0.48$). Coagulation and SOA condensation will increase $\overline{D_p}$ and OA evaporation will decrease $\overline{D_p}$. The plumes do not show significant changes in ΔOA/ΔCO (Fig. 2a), indicating that coagulation is likely responsible for the majority of increases in $\overline{D_p}$. The functional fits for Δf_{60} and Δf_{44} (Eq. 2; where X is $\overline{D_p}$ in this case) can also moderately predict $\overline{D_p}$ (R^2_p and R^2_s of 0.36 and 0.31; Fig. 3d) but do not well-predict $\Delta N_{40\text{-}300\ nm}/\Delta CO$ (not shown). Sakamoto et al. (2016) provide fit equations for modeled $\overline{D_p}$ as a function of age, but they include a known initial $\overline{D_p}$ at the time of emission in their parameterization, which is not available here. $\Delta N_{initial}$ in the place of $\Delta OA_{initial}$ in Eq. 2 predicts $\overline{D_p}$ similarly (Fig. S29). As discussed in Section 3.1, scatter in number concentrations limits our prediction skill.

Nucleation-mode particles (inferred in this study from particles appearing between 20-40 nm in the FIMS measurements) are observed for some of the transects (S7-S11). Some days also show nucleation-mode particles downwind of fires in between transects (Figs. S7, S8, S9, and S11). Nucleation-mode particles appear to primarily occur in the outer portion of plumes, although one day did show nucleation-mode particles within the core of the plume (Fig. S11). Nucleation at edges could be due to increased photooxidation from higher total irradiance relative to the core (Fig. S26). However, given the relatively small number of data points showing nucleation mode particles and limited photooxidation and gas-phase information, we do not have confidence in the underlying source of the nucleation-mode particles. The nucleation mode tends to be ~one order of magnitude less concentrated than the larger particles, and appears to be coagulating or evaporating away as the plumes travel downwind.

https://doi.org/10.5194/acp-2020-300
Preprint. Discussion started: 6 April 2020


Atmospheric Chemistry and Physics Discussions

4 Summary and outlook

The BBOP field campaign provided high time resolution (1 s) measurements of gas- and particle-phase smoke measurements downwind of western U.S. wildfires along pseudo-Lagrangian transects. These flights have allowed us to examine near-field (<4 hours) aging of smoke particles to provide analyses on how these species vary across a range of initial aerosol mass loadings (a proxy for the relative rates at which the plume is anticipated to dilute as dilution before the first observation is not a measurable quantity) as well as how they vary between the edges and cores of each plume. We find that although ΔOA/ΔCO shows little variability, Δf_{60} (a marker for evaporation) decreases with physical aging; Δf_{44} and ΔO/ΔC (markers for photochemical aging) increases with physical aging; and each correlate with both $\Delta OA_{initial}$ and physical age. $\Delta N_{40\text{-}262\ nm}/\Delta CO$ decreases with physical aging through coagulation, with thicker plumes tending to show lower number concentrations, indicative of higher rates of coagulation. Mean aerosol diameter between 40-262 nm increases with age primarily due to coagulation, as organic aerosol mass does not change significantly. Nucleation is observed within a few of the fires and appears to occur primarily on the edges of the plumes. Differences in initial values of Δf_{60}, Δf_{44}, and ΔO/ΔC between higher- and lower-concentrated plumes indicate that evaporation and/or chemistry has likely occurred before the time of initial measurement and that plumes or plume regions (such as the outer parts of the plume) with lower initial aerosol loading can undergo these changes more rapidly than thicker plumes. We encourage future studies to attempt to quantify these chemical and physical changes before the initial measurement using combinations of modeling and laboratory measurements, where sampling is possible at the initial stages of the fire and smoke. We also encourage future near-field (<24 hours) analyses of recent and future biomass burning field campaigns to include differences in initial plume mass concentrations and location within the plume as considerations for understanding chemical and physical processes in plumes.

Acknowledgements

We would like to thank Lauren Garofalo, Emily Fischer, Jakob Lindas, and Ilana Pollack for useful conversations. We thank Charles Long for use of irradiation data. This work is supported by the U.S. NOAA, an Office of Science, Office of Atmospheric Chemistry, Carbon Cycle, and Climate Program, under the cooperative agreement awards NA17OAR4310001 and NA17OAR4310003; the U.S. NSF Atmospheric Chemistry program, under Grants AGS-1559607 and AGS-1950327; and the US Department of Energy's (DOE) Atmospheric System Research, an Office of Science, Office of Biological and Environmental Research program, under grant DE-SC0019000. Work conducted by LIK, AJS, JW was performed under sponsorship of the U.S. DOE Office of Biological & Environmental Sciences (OBER) Atmospheric System Research Program (ASR) under contracts DE-SC0012704 (BNL; LIK, AJS) and DE-SC0020259 (JW). Researchers recognize the DOE Atmospheric Radiation Measurement (ARM) Climate Research program and facility for both the support to carry out the BBOP campaign and for use of the G-1 research aircraft. TBO acknowledges support from the DOE ARM program

https://doi.org/10.5194/acp-2020-300
Preprint. Discussion started: 6 April 2020

Atmospheric Chemistry and Physics Discussions

325 during BBOP and the DOE ASR program for BBOP analysis (contract DE-SC0014287). DKF acknowledges funding from NOAA Climate Program Office's Atmospheric Chemistry, Carbon Cycle, and Climate program (Grant NA17OAR4310010).

330 **References**

Adachi, K., Sedlacek, A. J., Kleinman, L., Springston, S. R., Wang, J. and Chand, D.: Spherical tarball particles form through rapid chemical and physical changes of organic matter in biomass-burning smoke, Proceedings of the National Academy of Sciences, 1–6, 2019.

Aiken, A. C., Decarlo, P. F., Kroll, J. H., Worsnop, D. R., Huffman, J. A., Docherty, K. S., Ulbrich, I. M., Mohr, C., 335 Kimmel, J. R., Sueper, D., Sun, Y., Zhang, Q., Trimborn, A., Northway, M., Ziemann, P. J., Canagaratna, M. R., Onasch, T. B., Alfarra, M. R., Prevot, A. S. H., Dommen, J., Duplissy, J., Metzger, A., Baltensperger, U. and Jimenez, J. L.: O/C and OM/OC ratios of primary, secondary, and ambient organic aerosols with high-resolution time-of-flight aerosol mass spectrometry, Environmental Science and Technology, 42(12), 4478–4485, 2008.

Aiken, A. C., Salcedo, D., Cubison, M. J., Huffman, J. A., DeCarlo, P. F., Ulbrich, I. M., Docherty, K. S., Sueper, D., 340 Kimmel, J. R., Worsnop, D. R. and Others: Mexico City aerosol analysis during MILAGRO using high resolution aerosol mass spectrometry at the urban supersite (T0)--Part 1: Fine particle composition and organic source apportionment, Atmos. Chem. Phys., 9(17), 6633–6653, 2009.

Akagi, S. K., Yokelson, R. J., Wiedinmyer, C., Alvarado, M. J., Reid, J. S., Karl, T., Crounse, J. D. and Wennberg, P. O.: Emission factors for open and domestic biomass burning for use in atmospheric models, Atmos. Chem. Phys., 345 11(9), 4039–4072, 2011.

Akagi, S. K., Craven, J. S., Taylor, J. W., Mcmeeking, G. R., Yokelson, R. J., Burling, I. R., Urbanski, S. P., Wold, C. E., Seinfeld, J. H., Coe, H., Alvarado, M. J. and Weise, D. R.: Evolution of trace gases and particles emitted by a chaparral fire in California, Atmos. Chem. Phys., 12, 1397–1421, 2012.

Albrecht, B. A.: Aerosols, cloud microphysics, and fractional cloudiness, Science, 245(4923), 1227–1230, 1989.

350 Alfarra, M. R., Coe, H., Allan, J. D., Bower, K. N., Boudries, H., Canagaratna, M. R., Jimenez, J. L., Jayne, J. T., Garforth, A. A., Li, S.-M. and Worsnop, D. R.: Characterization of urban and rural organic particulate in the Lower Fraser Valley using two Aerodyne Aerosol Mass Spectrometers, Atmos. Environ., 38(34), 5745–5758, 2004.

Andela, N., Morton, D. C., Giglio, L., Paugam, R., Chen, Y., Hantson, S., Werf, G. R. and Randerson, J. T.: The Global Fire Atlas of individual fire size, duration, speed and direction, Earth System Science Data, 11(2), 529–552, 2019.

https://doi.org/10.5194/acp-2020-300
Preprint. Discussion started: 6 April 2020


Atmospheric Chemistry and Physics Discussions

Badosa, J., Wood, J., Blanc, P., Long, C. N., Vuilleumier, L., Demengel, D. and Haeffelin, M.: Solar irradiances measured using SPN1 radiometers: uncertainties and clues for development, Atmospheric Measurement Techniques, 7, 4267–4283, 2014.

Bian, Q., Jathar, S. H., Kodros, J. K., Barsanti, K. C., Hatch, L. E., May, A. A., Kreidenweis, S. M. and Pierce, J. R.: Secondary organic aerosol formation in biomass-burning plumes: Theoretical analysis of lab studies and ambient plumes, Atmos. Chem. Phys., 17(8), 5459–5475, 2017.

Brito, J., Rizzo, L. V., Morgan, W. T., Coe, H., Johnson, B., Haywood, J., Longo, K., Freitas, S., Andreae, M. O. and Artaxo, P.: Ground-based aerosol characterization during the South American Biomass Burning Analysis (SAMBBA) field experiment, Atmospheric Chemistry and Physics, 14(22), 12069–12083, doi:10.5194/acp-14-12069-2014, 2014.

Cachier, H., Liousse, C., Buat-Menard, P. and Gaudichet, A.: Particulate content of savanna fire emissions, J. Atmos. Chem., 22(1-2), 123–148, 1995.

Canagaratna, M. R., Jimenez, J. L., Kroll, J. H., Chen, Q., Kessler, S. H., Massoli, P., Hildebrandt Ruiz, L., Fortner, E., Williams, L. R., Wilson, K. R. and Others: Elemental ration measurements of organic compounds using aerosol mass spectrometry: characterization, improved calibration, and implications, Atmos. Chem. Phys., 15, 253–272, 2015.

Capes, G., Johnson, B., McFiggans, G., Williams, P. I., Haywood, J. and Coe, H.: Aging of biomass burning aerosols over West Africa: Aircraft measurements of chemical composition, microphysical properties, and emission ratios, J. Geophys. Res. D: Atmos., 113(23), 0–15, 2008.

Cappa, C. D. and Jimenez, J. L.: Quantitative estimates of the volatility of ambient organic aerosol, Atmos. Chem. Phys., 10(12), 5409–5424, 2010.

Cappa, C. D. and Wilson, K. R.: Multi-generation gas-phase oxidation, equilibrium partitioning, and the formation and evolution of secondary organic aerosol, Atmos. Chem. Phys., 12(20), 9505–9528, 2012.

Carrico, C. M., Petters, M. D., Kreidenweis, S. M., Collett, J. L., Jr., Engling, G. and Malm, W. C.: Aerosol hygroscopicity and cloud droplet activation of extracts of filters from biomass burning experiments, J. Geophys. Res., 113(D8), 4767, 2008.

Collier, S., Zhou, S., Onasch, T. B., Jaffe, D. A., Kleinman, L., Sedlacek, A. J., Briggs, N. L., Hee, J., Fortner, E., Shilling, J. E., Worsnop, D., Yokelson, R. J., Parworth, C., Ge, X., Xu, J., Butterfield, Z., Chand, D., Dubey, M. K., Pekour, M. S., Springston, S. and Zhang, Q.: Regional Influence of Aerosol Emissions from Wildfires Driven by Combustion Efficiency: Insights from the BBOP Campaign, Environmental Science and Technology, 50(16), 8613–8622, 2016.

Cubison, M. J., Ortega, A. M., Hayes, P. L., Farmer, D. K., Day, D., Lechner, M. J., Brune, W. H., Apel, E., Diskin, G. S., Fisher, J. A., Fuelberg, H. E., Hecobian, A., Knapp, D. J., Mikoviny, T., Riemer, D., Sachse, G. W., Sessions, W., Weber, R. J., Weinheimer, A. J., Wisthaler, A. and Jimenez, J. L.: Effects of aging on organic aerosol from open biomass burning smoke in aircraft and laboratory studies, Atmos. Chem. Phys., 11(23), 12049–12064, 2011.

Decarlo, P. F., Dunlea, E. J., Kimmel, J. R., Aiken, A. C., Sueper, D., Crounse, J., Wennberg, P. O., Emmons, L., Shinozuka, Y., Clarke, A., Zhou, J., Tomlinson, J., Collins, D. R., Knapp, D., Weinheimer, A. J., Montzka, D. D., Campos, T. and Jimenez, J. L.: Fast airborne aerosol size and chemistry measurements above Mexico City and Central Mexico during the MILAGRO campaign., 2008.

Dennison, P. E., Brewer, S. C., Arnold, J. D. and Moritz, M. A.: Large wildfire trends in the western United States, 1984-2011, Geophysical Research Letters, 41(8), 2928–2933, doi:10.1002/2014gl059576, 2014.

Eatough, D. J., Eatough, N. L., Pang, Y., Sizemore, S., Kirchstetter, T. W., Novakov, T. and Hobbs, P. V.: Semivolatile particulate organic material in southern Africa during SAFARI 2000, J. Geophys. Res. D: Atmos., 108(D13) [online] Available from: https://agupubs.onlinelibrary.wiley.com/doi/abs/10.1029/2002JD002296%4010.1002/%28ISSN%292169-8996.SAF1, 2003.

Ford, B., Val Martin, M., Zelasky, S. E., Fischer, E. V., Anenberg, S. C., Heald, C. L. and Pierce, J. R.: Future Fire Impacts on Smoke Concentrations, Visibility, and Health in the Contiguous United States, GeoHealth, doi:10.1029/2018GH000144, 2018.

Formenti, P., Elbert, W., Maenhaut, W., Haywood, J., Osborne, S. and Andreae, M. O.: Inorganic and carbonaceous aerosols during the Southern African Regional Science Initiative (SAFARI 2000) experiment: Chemical characteristics, physical properties, and emission data for smoke from African biomass burning, J. Geophys. Res. D: Atmos., 108(D13), doi:10.1029/2002JD002408, 2003.

Forrister, H., Liu, J., Scheuer, E., Dibb, J., Ziemba, L., Thornhill, K. L., Anderson, B., Diskin, G., Perring, A. E., Schwarz, J. P., Campuzano-Jost, P., Day, D. A., Palm, B. B., Jimenez, J. L., Nenes, A. and Weber, R. J.: Evolution of brown carbon in wildfire plumes, Geophys. Res. Lett., 42(11), 4623–4630, 2015.

Gan, R. W., Ford, B., Lassman, W., Pfister, G., Vaidyanathan, A., Fischer, E., Volckens, J., Pierce, J. R. and Magzamen, S.: Comparison of wildfire smoke estimation methods and associations with cardiopulmonary-related hospital admissions, GeoHealth, 1(3), 122–136, 2017.

Garofalo, L., Pothier, M. A., Levin, E. J. T., Campos, T., Kreidenweis, S. M. and Farmer, D. K.: Emission and Evolution of Submicron Organic Aerosol in Smoke from Wildfires in the Western United States, ACS Earth and Space Chemistry, acsearthspacechem.9b00125, 2019.

Giglio, L., Csiszar, I. and Justice, C. O.: Global distribution and seasonality of active fires as observed with the Terra and Aqua Moderate Resolution Imaging Spectroradiometer (MODIS) sensors, Journal of Geophysical Research: Biogeosciences, 111(G2) [online] Available from: https://agupubs.onlinelibrary.wiley.com/doi/abs/10.1029/2005JG000142, 2006.

Giglio, L., Csiszar, I., Restás, Á., Morisette, J. T., Schroeder, W., Morton, D. and Justice, C. O.: Active fire detection and characterization with the advanced spaceborne thermal emission and reflection radiometer (ASTER), Remote Sensing of Environment, 112(6), 3055–3063, doi:10.1016/j.rse.2008.03.003, 2008.

https://doi.org/10.5194/acp-2020-300
Preprint. Discussion started: 6 April 2020

Gilman, J. B., Lerner, B. M., Kuster, W. C., Goldan, P. D., Warneke, C., Veres, P. R., Roberts, J. M., De Gouw, J. A., Burling, I. R. and Yokelson, R. J.: Biomass burning emissions and potential air quality impacts of volatile organic compounds and other trace gases from fuels common in the US, Atmos. Chem. Phys., 15(24), 13915–13938, 2015.

Hatch, L. E., Luo, W., Pankow, J. F., Yokelson, R. J., Stockwell, C. E. and Barsanti, K. C.: Identification and quantification of gaseous organic compounds emitted from biomass burning using two-dimensional gas chromatography-time-of-flight mass spectrometry, Atmos. Chem. Phys., 15(4), 1865–1899, 2015.

Hatch, L. E., Yokelson, R. J., Stockwell, C. E., Veres, P. R., Simpson, I. J., Blake, D. R., Orlando, J. J. and Barsanti, K. C.: Multi-instrument comparison and compilation of non-methane organic gas emissions from biomass burning and implications for smoke-derived secondary organic aerosol precursors, Atmos. Chem. Phys., 17, 1471–1489, 2017.

Heald, C. L., Kroll, J. H., Jimenez, J. L., Docherty, K. S., DeCarlo, P. F., Aiken, A. C., Chen, Q., Martin, S. T., Farmer, D. K. and Artaxo, P.: A simplified description of the evolution of organic aerosol composition in the atmosphere, Geophys. Res. Lett., 37(8), doi:10.1029/2010GL042737, 2010.

Hecobian, A., Liu, Z., Hennigan, C. J., Huey, L. G., Jimenez, J. L., Cubison, M. J., Vay, S., Diskin, G. S., Sachse, G. W., Wisthaler, A., Mikoviny, T., Weinheimer, A. J., Liao, J., Knapp, D. J., Wennberg, P. O., Urten, A., Crounse, J. D., Clair, J. S., Wang, Y. and Weber, R. J.: Comparison of chemical characteristics of 495 biomass burning plumes intercepted by the NASA DC-8 aircraft during the ARCTAS/CARB-2008 field campaign, Atmos. Chem. Phys., 11, 13325–13337, 2011.

Hobbs, P. V., Sinha, P., Yokelson, R. J., Christian, T. J., Blake, D. R., Gao, S., Kirchstetter, T. W., Novakov, T. and Pilewskie, P.: Evolution of gases and particles from a savanna fire in South Africa, J. Geophys. Res. D: Atmos., 108(D13), doi:10.1029/2002JD002352, 2003.

Hodshire, A. L., Akherati, A., Alvarado, M. J., Brown-Steiner, B., Jathar, S. H., Jimenez, J. L., Kreidenweis, S. M., Lonsdale, C. R., Onasch, T. B., Ortega, A. M. and Pierce, J. R.: Aging Effects on Biomass Burning Aerosol Mass and Composition: A Critical Review of Field and Laboratory Studies, Environ. Sci. Technol., 53(17), 10007–10022, 2019a.

Hodshire, A. L., Bian, Q., Ramnarine, E., Lonsdale, C. R., Alvarado, M. J., Kreidenweis, S. M., Jathar, S. H. and Pierce, J. R.: More than emissions and chemistry: Fire size, dilution, and background aerosol also greatly influence near-field biomass burning aerosol aging, J. Geophys. Res. D: Atmos., 2018JD029674, 2019b.

Huffman, J. A., Docherty, K. S., Aiken, A. C., Cubison, M. J., Ulbrich, I. M., Decarlo, P. F., Sueper, D., Jayne, J. T., Worsnop, D. R., Ziemann, P. J. and Jimenez, J. L.: Chemically-resolved aerosol volatility measurements from two megacity field studies., 2009.

Janhäll, S., Andreae, M. O. and Pöschl, U.: Biomass burning aerosol emissions from vegetation fires: particle number and mass emission factors and size distributions, Atmos. Chem. Phys. Disc., 9(4), 17183–17217, 2009.

https://doi.org/10.5194/acp-2020-300
Preprint. Discussion started: 6 April 2020


Atmospheric Chemistry and Physics Discussions

Jen, C. N., Hatch, L. E., Selimovic, V., Yokelson, R. J., Weber, R., Fernandez, A. E., Kreisberg, N. M., Barsanti, K. C. and Goldstein, A. H.: Speciated and total emission factors of particulate organics from burning western US wildland fuels and their dependence on combustion efficiency, Atmos. Chem. Phys., 19, 1013–1026, 2019.

Jimenez, J. L., Canagaratna, M. R., Donahue, N. M., Prevot, a. S. H., Zhang, Q., Kroll, J. H., DeCarlo, P. F., Allan, J. D., Coe, H., Ng, N. L., Aiken, a. C., Docherty, K. S., Ulbrich, I. M., Grieshop, a. P., Robinson, a. L., Duplissy, J., Smith, J. D., Wilson, K. R., Lanz, V. a., Hueglin, C., Sun, Y. L., Tian, J., Laaksonen, A., Raatikainen, T., Rautiainen, J., Vaattovaara, P., Ehn, M., Kulmala, M., Tomlinson, J. M., Collins, D. R., Cubison, M. J., Dunlea, E. J., Huffman, J. a., Onasch, T. B., Alfarra, M. R., Williams, P. I., Bower, K., Kondo, Y., Schneider, J., Drewnick, F., Borrmann, S., Weimer, S., Demerjian, K., Salcedo, D., Cottrell, L., Griffin, R., Takami, A., Miyoshi, T., Hatakeyama, S., Shimono, A., Sun, J. Y., Zhang, Y. M., Dzepina, K., Kimmel, J. R., Sueper, D., Jayne, J. T., Herndon, S. C., Trimborn, a. M., Williams, L. R., Wood, E. C., Middlebrook, a. M., Kolb, C. E., Baltensperger, U. and Worsnop, D. R.: Evolution of organic aerosols in the atmosphere, Science, 326(5959), 1525–1529, 2009.

Jolleys, M. D., Coe, H., McFiggans, G., Capes, G., Allan, J. D., Crosier, J., Williams, P. I., Allen, G., Bower, K. N., Jimenez, J. L., Russell, L. M., Grutter, M. and Baumgardner, D.: Characterizing the aging of biomass burning organic aerosol by use of mixing ratios: A meta-analysis of four regions, Environmental Science and Technology, 46(24), 13093–13102, 2012.

Jolleys, M. D., Coe, H., McFiggans, G., Taylor, J. W., O'Shea, S. J., Le Breton, M., Bauguitte, S. J. B., Moller, S., Di Carlo, P., Aruffo, E., Palmer, P. I., Lee, J. D., Percival, C. J. and Gallagher, M. W.: Properties and evolution of biomass burning organic aerosol from Canadian boreal forest fires, Atmos. Chem. Phys., 15(6), 3077–3095, 2015.

Kleinman, L. and Sedlacek, A. J., III: Biomass Burning Observation Project (BBOP) Final Campaign Report, 2016.

Kleinman, L. I., Sedlacek, A. J., III, Adachi, K., Buseck, P. R., Collier, S., Dubey, M., K., Hodshire, A. L., Lewis, E., Onasch, T. B., Pierce, J. R., Schilling, J., Springston, S. R., Wang, J., Zhang, Q., Zhoui, S., Yokelson, R. J.: Rapid Evolution of Aerosol Particles and their Optical Properties Downwind of Wildfires in the Western U.S., submitted to Atmos. Chem. Phys., 2020.

Konovalov, I. B., Beekmann, M., Golovushkin, N. A. and Andreae, M. O.: Nonlinear behavior of organic aerosol in biomass burning plumes: a microphysical model analysis, Atmos. Chem. Phys. Disc., 1–44, 2019.

Koss, A. R., Sekimoto, K., Gilman, J. B., Selimovic, V., Coggon, M. M., Zarzana, K. J., Yuan, B., Lerner, B. M., Brown, S. S., Jimenez, J. L., Krechmer, J., Roberts, J. M., Warneke, C., Yokelson, R. J. and De Gouw, J.: Non-methane organic gas emissions from biomass burning: Identification, quantification, and emission factors from PTR-ToF during the FIREX 2016 laboratory experiment, Atmos. Chem. Phys., 18(5), 3299–3319, 2018.

Kroll, J. H. and Seinfeld, J. H.: Chemistry of secondary organic aerosol: Formation and evolution of low-volatility organics in the atmosphere, Atmos. Environ., 42, 3593–3624, 2008.

Kulkarni, P. and Wang, J.: New fast integrated mobility spectrometer for real-time measurement of aerosol size distribution—I: Concept and theory, J. Aerosol Sci., 37(10), 1303–1325, 2006.

https://doi.org/10.5194/acp-2020-300
Preprint. Discussion started: 6 April 2020


Atmospheric Chemistry and Physics Discussions

Lee, T., Sullivan, A. P., Mack, L., Jimenez, J. L., Kreidenweis, S. M., Onasch, T. B., Worsnop, D. R., Malm, W., Wold, C. E., Hao, W. M. and Collett, J. L.: Chemical Smoke Marker Emissions During Flaming and Smoldering Phases of Laboratory Open Burning of Wildland Fuels, Aerosol Sci. Technol., 44(9), i–v, 2010.

Liu, X., Zhang, Y., Huey, L. G., Yokelson, R. J., Wang, Y., Jimenez, J. L., Campuzano-Jost, P., Beyersdorf, A. J., Blake, D. R., Choi, Y., St. Clair, J. M., Crounse, J. D., Day, D. A., Diskin, G. S., Ried, A., Hall, S. R., Hanisco, T. F., King, L. E., Meinardi, S., Mikoviny, T., Palm, B. B., Peischl, J., Perring, A. E., Pollack, I. B., Ryerson, T. B., Sachse, G., Schwarz, J. P., Simpson, I. J., Tanner, D. J., Thornhil, K. L., Ullmann, K., Weber, R. J., Wennberg, P. O., Wisthaler, A., Wolfe, G. M. and Ziemba, L. D.: Agricultural fires in the southeastern U.S. during SEAC4RS: Emissions of trace gases and particles and evolution of ozone, reactive nitrogen, and organic aerosol, J. Geophys. Res., 121(12), 7383–7414, 2016.

Long, C. N., Bucholtz, A., Jonsson, H., Schmid, B., Vogelmann, A. and Wood, J.: A Method of Correcting for Tilt from Horizontal in Downwelling Shortwave Irradiance Measurements on Moving Platforms, The Open Atmospheric Science Journal, 4(1), 78–87, doi:10.2174/1874282301004010078, 2010.

May, A. A., Levin, E. J. T., Hennigan, C. J., Riipinen, I., Lee, T., Collett, J. L., Jimenez, J. L., Kreidenweis, S. M. and Robinson, A. L.: Gas-particle partitioning of primary organic aerosol emissions: 3. Biomass burning, J. Geophys. Res. D: Atmos., 118(19), 11327–11338, 2013.

May, A. A., Lee, T., McMeeking, G. R., Akagi, S., Sullivan, A. P., Urbanski, S., Yokelson, R. J. and Kreidenweis, S. M.: Observations and analysis of organic aerosol evolution in some prescribed fire smoke plumes, Atmos. Chem. Phys., 15(11), 6323–6335, 2015.

Morgan, W. T., Allan, J. D., Bauguitte, S., Darbyshire, E., Flynn, M. J., Lee, J., Liu, D., Johnson, B., Haywood, J., Longo, K. M., Artaxo, P. E. and Coe, H.: Transformation and aging of biomass burning carbonaceous aerosol over tropical South America from aircraft in-situ measurements during SAMBBA, Atmos. Chem. Phys. Discuss., doi:10.5194/acp-2019-157, 2019.

Moteki, N. and Kondo, Y.: Dependence of Laser-Induced Incandescence on Physical Properties of Black Carbon Aerosols: Measurements and Theoretical Interpretation, Aerosol Sci. Technol., 44(8), 663–675, 2010.

Nance, J. D., Hobbs, P. V. and Radkel, L. F.: Airborne Measurements of Gases and Particles From an Alaskan Wildfire, J. Geophys. Res. D: Atmos., 98(D8), 873–882, 1993.

Noyes, K. J., Kahn, R., Sedlacek, A., Kleinman, L., Limbacher, J. and Li, Z.: Wildfire Smoke Particle Properties and Evolution, from Space-Based Multi-Angle Imaging, Remote Sensing, 12(5), 769, doi:10.3390/rs12050769, 2020.

O'Dell, K., Ford, B., Fischer, E. V. and Pierce, J. R.: Contribution of Wildland-Fire Smoke to US PM2.5 and Its Influence on Recent Trends, Environmental Science & Technology, 53(4), 1797–1804, doi:10.1021/acs.est.8b05430, 2019.

Olfert, J. S. and Wang, J.: Dynamic Characteristics of a Fast-Response Aerosol Size Spectrometer, Aerosol Sci. Technol., 43(2), 97–111, 2009.

https://doi.org/10.5194/acp-2020-300
Preprint. Discussion started: 6 April 2020


Atmospheric Chemistry and Physics Discussions

Onasch, T. B., Trimborn, A., Fortner, E. C., Jayne, J. T., Kok, G. L., Williams, L. R., Davidovits, P. and Worsnop, D. R.: Soot Particle Aerosol Mass Spectrometer: Development, Validation, and Initial Application, Aerosol Science and Technology, 46(7), 804–817, doi:10.1080/02786826.2012.663948, 2012.

Petters, M. D. and Kreidenweis, S. M.: A single parameter representation of hygroscopic growth and cloud condensation nucleus activity, Atmos. Chem. Phys., 7(8), 1961–1971, 2007.

Petters, M. D., Carrico, C. M., Kreidenweis, S. M., Prenni, A. J., DeMott, P. J., Collett, J. L. and Moosmüller, H.: Cloud condensation nucleation activity of biomass burning aerosol, J. Geophys. Res. D: Atmos., 114(22), 22205, 2009.

Ramnarine, E., Kodros, J. K., Hodshire, A. L., Lonsdale, C. R., Alvarado, M. J. and Pierce, J. R.: Effects of near-source coagulation of biomass burning aerosols on global predictions of aerosol size distributions and implications for aerosol radiative effects, Atmos. Chem. Phys., 19(9), 6561–6577, 2019.

Reid, C. E., Brauer, M., Johnston, F. H., Jerrett, M., Balmes, J. R. and Elliott, C. T.: Critical review of health impacts of wildfire smoke exposure, Environmental Health Perspectives, 124(9), 1334–1343, doi:10.1289/ehp.1409277, 2016.

Reid, J. S., Hobbs, P. V., Ferek, R. J., Blake, D. R., Martins, J. V., Dunlap, M. R. and Liousse, C.: Physical, chemical, and optical properties of regional hazes dominated by smoke in Brazil, J. Geophys. Res. D: Atmos., 103(D24), 32059–32080, 1998.

Reid, J. S., Eck, T. F., Christopher, S. A., Koppmann, R., Dubovik, O., Eleuterio, D. P., Holben, B. N., Reid, E. A. and Zhang, J.: A review of biomass burning emissions part III: intensive optical properties of biomass burning particles, Atmos. Chem. Phys., 5, 827–849, 2005.

Sakamoto, K. M., Allan, J. D., Coe, H., Taylor, J. W., Duck, T. J. and Pierce, J. R.: Aged boreal biomass-burning aerosol size distributions from BORTAS 2011, Atmos. Chem. Phys., 15(4), 1633–1646, 2015.

Sakamoto, K. M., Laing, J. R., Stevens, R. G., Jaffe, D. A. and Pierce, J. R.: The evolution of biomass-burning aerosol size distributions due to coagulation: Dependence on fire and meteorological details and parameterization, Atmos. Chem. Phys., 16(12), 7709–7724, 2016.

Schwarz, J. P., Gao, R. S., Fahey, D. W., Thomson, D. S., Watts, L. A., Wilson, J. C., Reeves, J. M., Darbeheshti, M., Baumgardner, D. G., Kok, G. L. and Others: Single-particle measurements of midlatitude black carbon and light-scattering aerosols from the boundary layer to the lower stratosphere, J. Geophys. Res. D: Atmos., 111(D16) [online] Available from: https://agupubs.onlinelibrary.wiley.com/doi/abs/10.1029/2006JD007076, 2006.

Sedlacek, A. J., Iii, Buseck, P. R., Adachi, K., Onasch, T. B., Springston, S. R. and Kleinman, L.: Formation and evolution of Tar Balls from Northwestern US wildfires, Atmos. Chem. Phys. Discuss., (Figure 1), 1–28, 2018.

Seinfeld, J. H. and Pandis, S. N.: Atmospheric chemistry and physics: From air pollution to climate change, John Willey & Sons, Inc. , New York, 2006.

Shrivastava, M., Cappa, C. D., Fan, J., Goldstein, A. H., Guenther, A. B., Jimenez, J. L., Kuang, C., Laskin, A., Martin, S. T., Ng, N. L. and Others: Recent advances in understanding secondary organic aerosol: Implications for global climate forcing, Rev. Geophys., 55(2), 509–559, 2017.

https://doi.org/10.5194/acp-2020-300
Preprint. Discussion started: 6 April 2020

Spracklen, D. V., Mickley, L. J., Logan, J. A., Hudman, R. C., Yevich, R., Flannigan, M. D. and Westerling, A. L.: Impacts of climate change from 2000 to 2050 on wildfire activity and carbonaceous aerosol concentrations in the western United States, J. Geophys. Res., 114(D20), 1418, 2009.

Tang, X., Madronich, S., Wallington, T. and Calamari, D.: Changes in tropospheric composition and air quality, J. Photochem. Photobiol. B, 46(1-3), 83–95, 1998.

Tie, X.: Effect of clouds on photolysis and oxidants in the troposphere, J. Geophys. Res., 108(D20), 23,073, 2003.

Twomey, S.: Pollution and the planetary albedo, Atmos. Environ., 8(12), 1251–1256, 1974.

Vakkari, V., Kerminen, V.-M., Beukes, J. P., Titta, P., van Zyl, P. G., Josipovic, M., Wnter, A. D., Jaars, K., Worsnop, D. R., Kulmala, M. and Laakso, L.: Rapid changes in biomass burning aerosols by atmospheric oxidation, Geophys. Res. Lett., 2644–2651, 2014.

Vakkari, V., Beukes, J. P., Dal Maso, M., Aurela, M., Josipovic, M. and van Zyl, P. G.: Major secondary aerosol formation in southern African open biomass burning plumes, Nat. Geosci., 11(8), 580–583, 2018.

Volkamer, R., Jimenez, J. L., San Martini, F., Dzepina, K., Zhang, Q., Salcedo, D., Molina, L. T., Worsnop, D. R. and Molina, M. J.: Secondary organic aerosol formation from anthropogenic air pollution: Rapid and higher than expected, Geophys. Res. Lett., 33(17), 4407, 2006.

Volkamer, R., Ziemann, P. J. and Molina, M. J.: Secondary Organic Aerosol Formation from Acetylene (C2H2): seed effect on SOA yields due to organic photochemistry in the aerosol aqueous phase, Atmos. Chem. Phys., 9(6), 1907–1928, 2009.

Wang, J., -N. Lee, Y., Daum, P. H., Jayne, J. and Alexander, M. L.: Effects of aerosol organics on cloud condensation nucleus (CCN) concentration and first indirect aerosol effect, Atmospheric Chemistry and Physics, 8(21), 6325–6339, doi:10.5194/acp-8-6325-2008, 2008.

Yang, M., Blomquist, B. W. and Huebert, B. J.: Constraining the concentration of the hydroxyl radical in a stratocumulus-topped marine boundary layer from sea-to-air eddy covariance flux measurements of dimethylsulfide, Atmos. Chem. Phys., 9(23), 9225–9236, 2009.

Yokelson, R. J., Crounse, J. D., DeCarlo, P. F., Karl, T., Urbanski, S., Atlas, E., Campos, T., Shinozuka, Y., Kapustin, V., Clarke, A. D., Weinheimer, A., Knapp, D. J., Montzka, D. D., Holloway, J., Weibring, P., Flocke, F., Zheng, W., Toohey, D., Wennberg, P. O., Wiedinmyer, C., Mauldin, L., Fried, A., Richter, D., Walega, J., Jimenez, J. L., Adachi, K., Buseck, P. R., Hall, S. R. and Shetter, R.: Emissions from biomass burning in the Yucatan, Atmos. Chem. Phys., 9(15), 5785–5812, 2009.

Yue, X., Mickley, L. J., Logan, J. A. and Kaplan, J. O.: Ensemble projections of wildfire activity and carbonaceous aerosol concentrations over the western United States in the mid-21st century, Atmospheric Environment, 77, 767–780, doi:10.1016/j.atmosenv.2013.06.003, 2013.

https://doi.org/10.5194/acp-2020-300
Preprint. Discussion started: 6 April 2020

Atmospheric Chemistry and Physics Discussions

Zhou, S., Collier, S., Jaffe, D. A., Briggs, N. L., Hee, J., Sedlacek, A. J., III, Kleinman, L., Onasch, T. B. and Zhang, Q.: Regional influence of wildfires on aerosol chemistry in the western US and insights into atmospheric aging of biomass burning organic aerosol, Atmos. Chem. Phys., 17(3), 2477–2493, 2017.

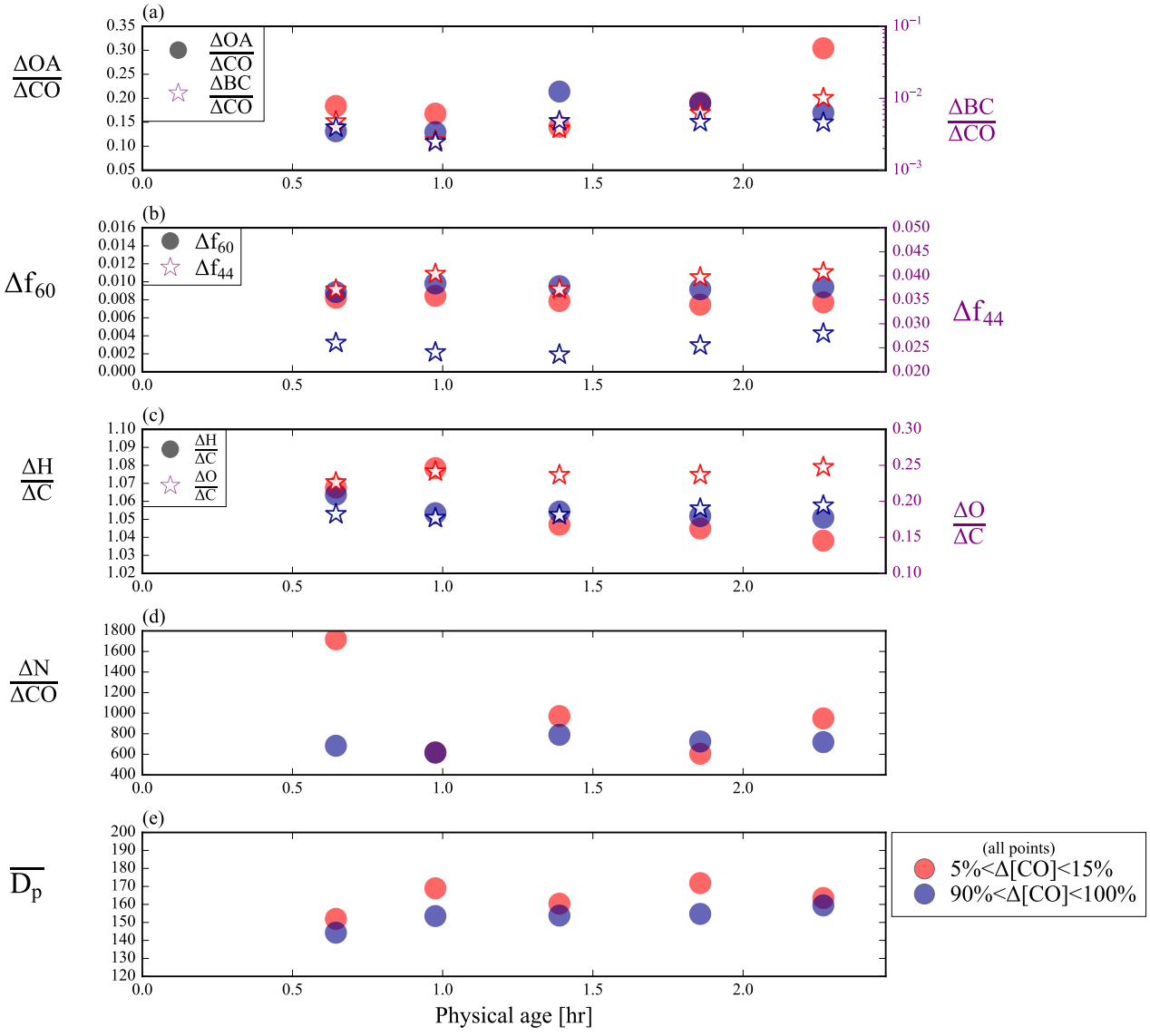

Figure 1: Aerosol properties from the first set of pseudo-Lagrangian transects from the Colockum fire on flight '730b' (a) ΔOA/ΔCO (right y-axis) and ΔrBC/ΔCO (left y-axis), (b) Δf_{60} (right y-axis) and Δf_{44} (left y-axis), (c) ΔH/ΔC (right y-axis) and

https://doi.org/10.5194/acp-2020-300
Preprint. Discussion started: 6 April 2020

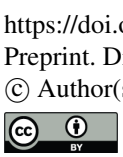

Atmospheric Chemistry and Physics Discussions

ΔO/ΔC (left y-axis), (d) ΔN/ΔCO, and (e) $\overline{D_p}$ against physical age. For each transect, the data is divided into edge (the lowest 5-15% of ΔCO data; red points) and core (90-100% of ΔCO data; blue points). ΔrBC/ΔCO is shown in log scale to improve clarity.

600

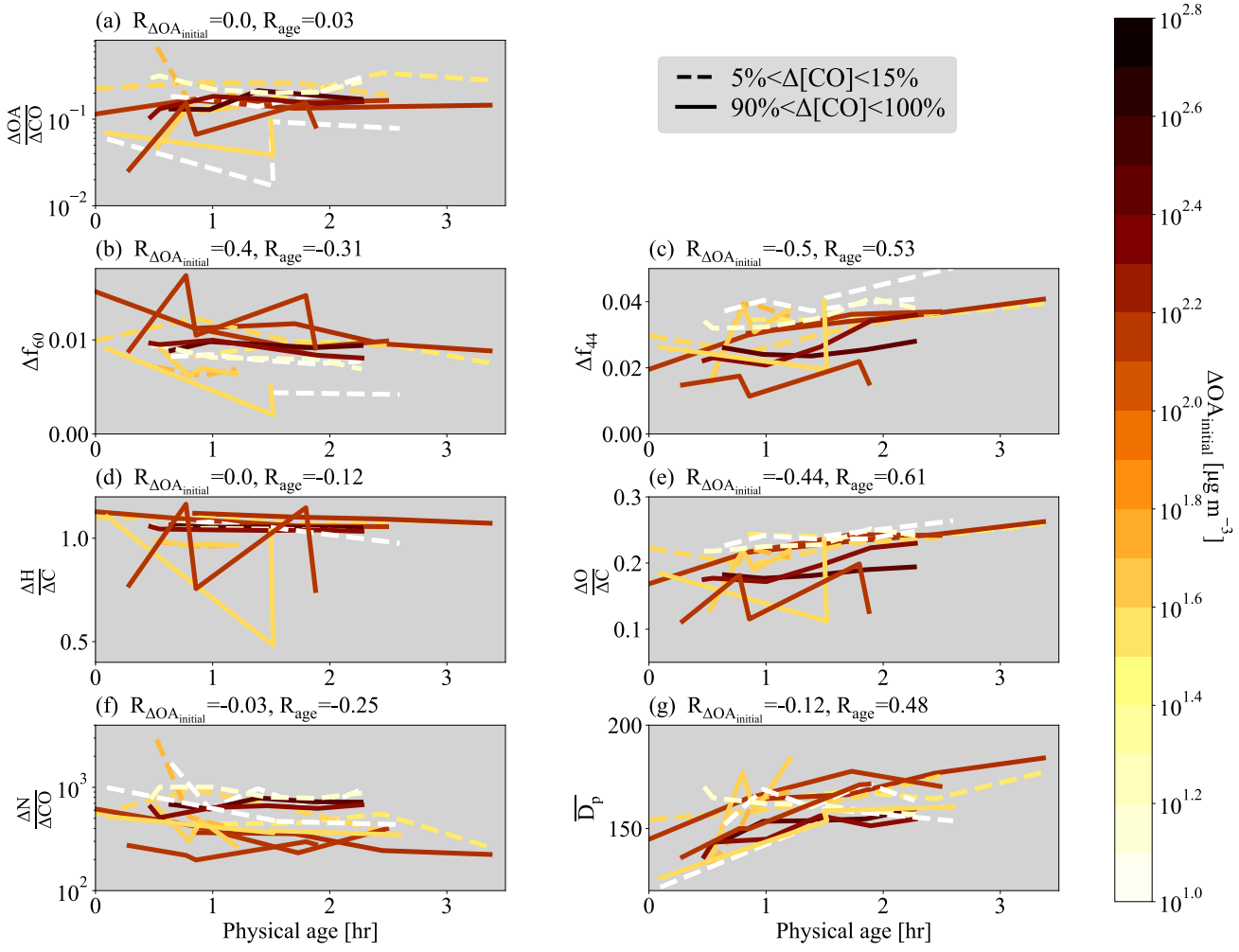

Figure 2. Various normalized parameters as a function of age for the 7 sets of pseudo-Lagrangian transects. Separate lines are shown for the edges (lowest 5-15% of ΔCO; dashed lines) and cores (highest 90-100% of ΔCO; solid lines). (a) ΔOA/ΔCO, (b) Δf_{60}, (c) Δf_{44}, (d) ΔH/ΔC, (e) ΔO/ΔC, (f) $\Delta N_{40\text{-}262\ nm}$/ΔCO, and (g) $\overline{D_p}$ between 40-262 nm against physical age for all flights, colored by $\Delta OA_{initial}$. Some flights have missing data. Also provided is the Spearman correlation coefficient, R, between each variable and $\Delta OA_{initial}$ and physical age for each variable. Note that panels (a), (d), and (g) have a log y-axis.

610

https://doi.org/10.5194/acp-2020-300
Preprint. Discussion started: 6 April 2020

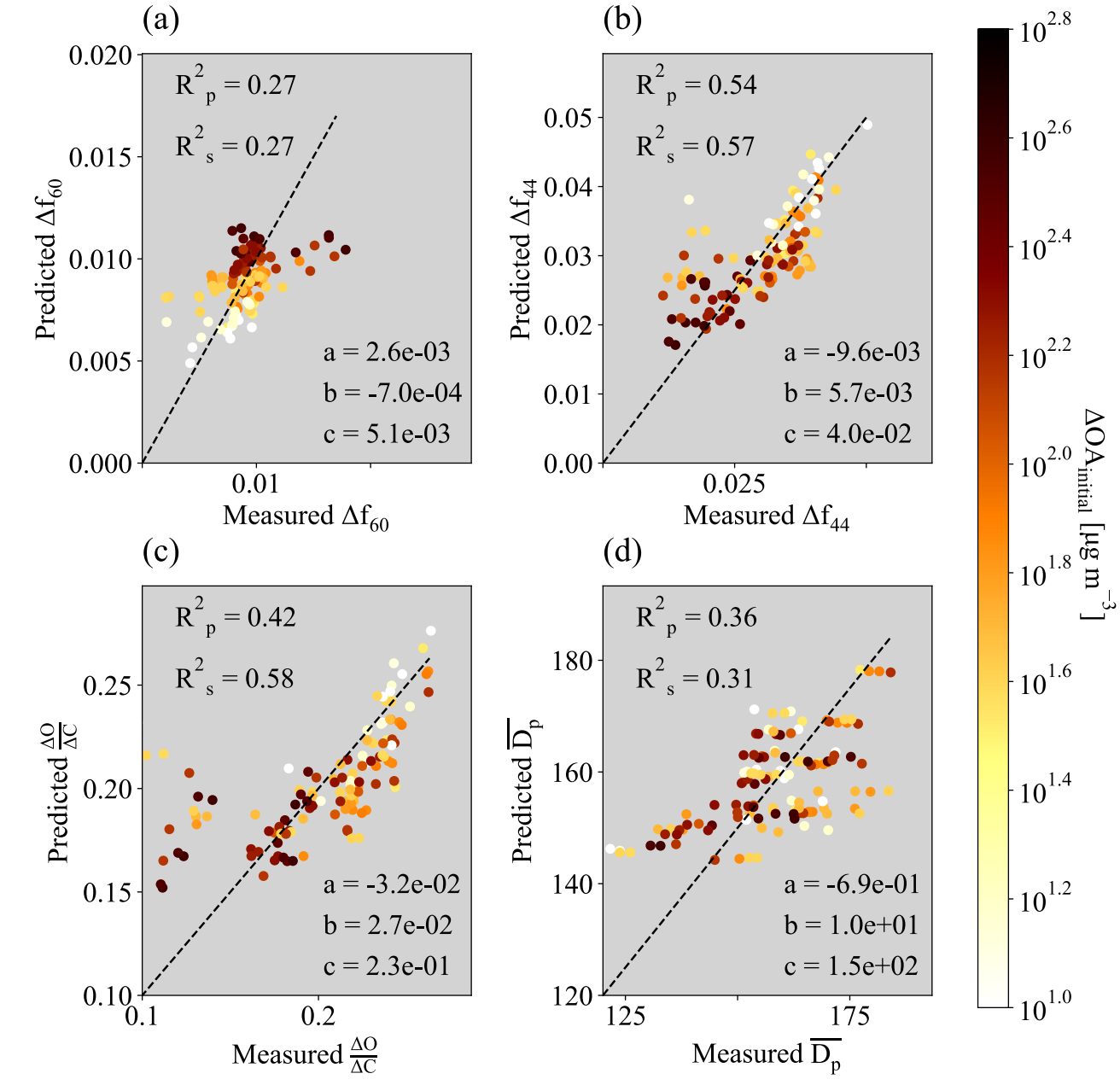

Figure 3. Measured versus predicted (a) Δf_{60}, (b) Δf_{44}, (c) ΔO/ΔC, and (d) $\overline{D_p}$ between 40-262 nm. The predicted values are from the equation $X = a\ log_{10}(OAinitial) + b\ (Physical\ age) + c$ where $X = \Delta f_{60}$, Δf_{44}, ΔO/ΔC, or $\overline{D_p}$. The values of *a*, *b*, and *c* are provided within each subpanel, as are the Pearson and Spearman coefficients of determination (R^2_p and R^2_s, respectively). Note that Fig. 2 provides R values rather than R^2 to provide information upon the trend of the correlation. Included in the fit and figure are points from all four ΔCO regions within the plume (the 5-15%, 15-50%, 50-90%, and 90-100% of ΔCO), all colored by the mean $\Delta OA_{initial}$ of each ΔCO percentile range.